

# Signal Waveforms and Range/Angle Coupling in Coherent Colocated MIMO Radar

Olivier Rabaste, Laurent Savy, Mathieu Cattenoz  
ONERA, The French Aerospace Lab  
BP 80100  
91123 Palaiseau Cedex, France

Jean-Paul Guyvarch  
Thales Air Systems  
3 avenue Charles Lindbergh  
94628 RUNGIS Cedex - France

**Abstract**—In this paper, we consider the coherent colocated MIMO radar framework. We show in this paper that the MIMO ambiguity function presents a range/angle coupling for any waveform family except for perfectly orthogonal families that are unrealistic in practice. We then propose a general model for intrapulse coded MIMO waveforms, and we exhibit different waveform families within this model. For each coding scheme, the MIMO ambiguity function is studied and the range/angle coupling characterized. We also compute the corresponding Cramer-Rao Lower-Bounds. Finally real measurements obtained from a MIMO radar permit to confirm the shape of the ambiguity functions for the studied waveforms.

## I. INTRODUCTION

Modern radar systems, for medium or long range applications, are generally based on active antennas, transmitting the signals generated by agile waveform synthesizers, and adaptively processing the received echoes, for extraction of targets from clutter and identification of potential threats.

Standard surveillance modes involve electronic scanning of a focused beam (Figure 1.a), successively exploring the directions of interest with a sequence of search waveforms (e.g. High Repetition Frequency bursts for long-range air-air search, Low Repetition Frequency bursts for surface-based radars), and removing ambiguities through comparison of the received signals for the successive bursts at different repetition frequencies and/or different wavelengths. Confirmation modes may also be interleaved between the standard scanning modes for improved detection probabilities in directions where elementary detections have been obtained.

Some modern radars also make use of a widened beam on transmit (Figure 1.b), allowing for longer illumination time and thus better extraction of targets, and combining multiple receiving antennas for digital beamforming of focused pencil-beams in parallel. This technique is for instance used for surface-based radar, with a wide elevation beam on transmit and so-called stacked beams on receive.

This paper deal with an alternative to these basic scanning or staring modes, called coherent co-located MIMO [1], [2], [3], [4]. It consists in space-time coding on transmit of each individual transmitters (or sub-arrays), allowing to identify each of them by a convenient processing on receive, and hence to recover the angular directivity of the whole antenna. From a radar functional point of view, everything appears as if the directions were explored simultaneously by coded

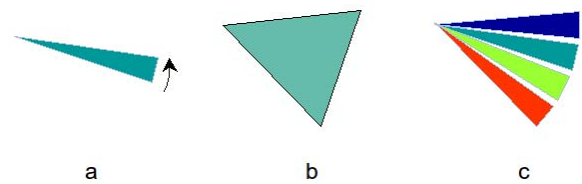


Fig. 1. Transmission beams: a) scanning pencil beam; b) wide beam; c) multiple simultaneous coded beams.

focused beams, as shown on (Figure 1.c), allowing a wide angle domain to be explored instantaneously, without loss of transmit directivity as with classical wide beam illumination of Figure 1.b. It is worth noting that this coherent MIMO has nothing to do with non-coherent (or statistical) MIMO, that mainly exploits spatial diversity on target, using well separated (multistatic, non-colocated) transmitting antennas [5], [6]. Coherent co-located MIMO is the only mean for a radar to obtain an ultra-wide angular beam on transmit (more than the classical factor 3 or 4 compared to the focused beamwidth) with good sidelobe and mainlobe properties (ripple, sidelobe level). Ultra wide beam are required for instance for transitory targets (helicopter pop-up, periscope), or slow small moving targets in competition with clutter and/or strong targets.

The coherent processing on receive is obtained via a general matched filter in range, angles and Doppler. The corresponding MIMO ambiguity function which represents the output of the MIMO processing for a given set of transmitted signals, can be derived. It is an interesting tool to characterize different waveform families. This MIMO ambiguity function has been extensively and theoretically defined and studied in [7], [3], [8]. However most of the properties stated are obtained under the assumption that the transmitted waveforms are perfectly orthogonal for any (angle-range-doppler) target hypothesis. In other words, in most cases authors do not consider the problem induced by the range sidelobes and/or the spreading of the signal energy in the range/angle plane, even though these sidelobes may present a strong level. However these sidelobes are of critical importance for the radar detection problem.

In this paper, we show that the MIMO ambiguity function exhibits a range/angle coupling as soon as the transmitted waveforms are not perfectly orthogonal, where the orthogo-

nality is considered for any waveform and any time delay values between the waveforms. Note that it is not possible to find a set of waveform that satisfies this orthogonality, so that range coupling will always occur in practice. We then propose a general model for describing MIMO waveforms and we present different possible families of waveforms that can be used in coherent MIMO radars. For each family, we present the specificity of the observed range/angle coupling. It comes that, while for some waveform families the range/angle coupling is approximately uniformly spread in the range/angle plane, for some other waveform families it may be concentrated in specific areas, even though the considered waveforms are all orthogonal for the zero time delay. The computation of Cramer-Rao Lower-Bound ellipses permits to quantify the distortion of the ambiguity mainlobe. Finally, in order to check the validity of the theoretical ambiguity function presented here, a real experiment was conducted using a MIMO radar demonstrator. The ambiguity functions obtained with these real measurements fairly match the theoretical ones.

## II. COHERENT MIMO AMBIGUITY FUNCTION

In this paper, we consider a transmitting array of  $N_E$  antennas and a receiving array composed of  $N_R$  antennas. The position of the  $m^{\text{th}}$  antenna of the transmitting array is denoted by vector  $\mathbf{x}_{E,m}$  while the position of the  $n^{\text{th}}$  antenna of the receiving array is given by vector  $\mathbf{x}_{R,n}$ . We assume that the transmitting and receiving arrays are colocated. Of course, in a more general setting, subarrays could be considered in place of single antennas.

### A. Expression of the MIMO ambiguity function

In the coherent colocated MIMO framework, all elementary antennas (or subarrays) of the transmitting array transmit different waveforms. Denoting by  $s_m(t)$  the waveform assigned to the  $m^{\text{th}}$  antenna, the signal transmitted by the array is

$$s(t, \theta) = \sum_{m=0}^{N_E-1} g_m^E(\theta) e^{j\mathbf{x}_{E,m}^T \mathbf{k}(\theta)} s_m(t),$$

where  $\theta$  is the considered direction,  $\mathbf{k}(\theta)$  is the wave vector,  $g_m^E(\theta)$  is the gain of transmitting subarray  $m$  in direction  $\theta$  and the notation  $\cdot^T$  represents the matrix transpose. If a target is present in direction  $\theta_c$  with delay  $\tau_c$  and doppler  $\nu_c$ , then the signal received on the  $n^{\text{th}}$  antenna is:

$$s_n^r(t) = g_n^R(\theta_c) e^{j\mathbf{x}_{R,n}^T \mathbf{k}(\theta_c)} \sum_{m=0}^{N_E-1} g_m^E(\theta_c) e^{j\mathbf{x}_{E,m}^T \mathbf{k}(\theta_c)} s_m(t - \tau_c) e^{j2\pi\nu_c t},$$

where  $g_n^R(\theta_c)$  is the gain of receiving subarray  $n$  in direction  $\theta_c$ . Concatenating signals  $s_n^r(t)$  from all receiving antennas in a single vector  $\mathbf{s}^r(t) = [s_0^r(t), s_1^r(t), \dots, s_{N_R-1}^r(t)]^T$ , and transmitted waveforms  $s_m(t)$  in a single vector  $\mathbf{s}(t) = [s_0(t), s_1(t), \dots, s_{N_E-1}(t)]^T$ , we get:

$$\mathbf{s}^r(t) = \mathbf{s}_R(\theta_c) (\mathbf{s}_E(\theta_c)^T \mathbf{s}(t - \tau_c) e^{j2\pi\nu_c t}),$$

where  $\mathbf{s}_R(\theta)$  and  $\mathbf{s}_E(\theta)$  are the steering vectors for transmission and reception, whose  $n^{\text{th}}$  elements are given by:

$$(\mathbf{s}_R(\theta))_n = g_n^R(\theta) e^{j\mathbf{x}_{R,n}^T \mathbf{k}(\theta)} \text{ and } (\mathbf{s}_E(\theta))_n = g_n^E(\theta) e^{j\mathbf{x}_{E,n}^T \mathbf{k}(\theta)}.$$

The optimal coherent MIMO processing on receive, where we have skipped for simplicity the antenna gains, is given by:

$$r(\tau, \nu, \theta) = \underbrace{\sum_{n=0}^{N_R-1} e^{-j\mathbf{x}_{R,n}^T \mathbf{k}(\theta)}}_{\text{Beamforming on receive}} \underbrace{\sum_{m'=0}^{N_E-1} e^{-j\mathbf{x}_{E,m'}^T \mathbf{k}(\theta)}}_{\text{Beamforming on transmit}} \times \underbrace{\int s_n^r(t) s_{m'}^*(t + \tau) e^{-j2\pi\nu t} dt}_{\text{Transmitter separation and range compression}} \quad (1)$$

Clearly this optimal processing can be decomposed into three steps: first, at each reception antenna, application of a filter matched to each transmitted waveforms (i.e.  $N_E$  matched filters applied to  $N_R$  received data, producing  $N_E N_R$  output data streams); second a transmission processing that permits to retrieve the transmission phase; third a reception processing that corresponds to the usual beamforming step.

Inserting the expression of  $s_n^r(t)$  in (1) and replacing  $\nu - \nu_c$  by  $\nu$  and  $\tau - \tau_c$  by  $\tau$  provides the MIMO ambiguity function given by [3]:

$$A(\tau, \nu, \theta, \theta_c) = \left( \sum_{n=0}^{N_R-1} e^{j\mathbf{x}_{R,n}^T (\mathbf{k}(\theta_c) - \mathbf{k}(\theta))} \right) \times \sum_{m'=0}^{N_E-1} \sum_{m=0}^{N_E-1} e^{j\mathbf{x}_{E,m}^T \mathbf{k}(\theta_c) - j\mathbf{x}_{E,m'}^T \mathbf{k}(\theta)} \int s_m(t) s_{m'}^*(t + \tau) e^{-j2\pi\nu t} dt, \quad (2)$$

which is a function of four parameters (delay, doppler, target angle, reception angle) if only one angle direction (azimuth or elevation) is considered. If two directions were considered, it would become a function of six parameters. Note that the target angle and the reception angle cannot be summarized by only one angle parameter because in coherent MIMO, signals received by two targets in two different directions differ.

Using the above vector notation, the ambiguity function can be rewritten in the following way:

$$A(\tau, \nu, \theta, \theta_c) = (\mathbf{s}_R^H(\theta) \mathbf{s}_R(\theta_c)) \times \mathbf{s}_E^T(\theta) \left( \int \mathbf{s}(t) \mathbf{s}^H(t + \tau) e^{-j2\pi\nu t} dt \right) \mathbf{s}_E^*(\theta_c),$$

where  $\mathbf{x}^H$  is the hermitian transpose of vector  $\mathbf{x}$ .

Since the reception processing is completely decoupled in equation (2), we may consider only the following expression, corresponding to the case of one single reception antenna:

$$A_e(\tau, \nu, \theta, \theta_c) = \mathbf{s}_E^T(\theta_c) \left( \int \mathbf{s}(t) \mathbf{s}^H(t + \tau) e^{-j2\pi\nu t} dt \right) \mathbf{s}_E^*(\theta). \quad (3)$$

For applications where the Doppler effect is negligible within the pulse duration, it can be decoupled in the expression (3). This is the case for instance for the detection of slow moving targets. For simplicity, we restrict our analysis to that approximation in the following, and (3) can be simplified further to:

$$A_e(\tau, \theta, \theta_c) = \mathbf{s}_E^T(\theta_c) \mathbf{S}(\tau) \mathbf{s}_E^*(\theta), \quad (4)$$

where

$$\mathbf{S}(\tau) = \int \mathbf{s}(t)\mathbf{s}^H(t + \tau) dt$$

is the matrix containing all the information about the auto and cross correlations of the transmitted waveforms.

Other theoretical properties of the MIMO ambiguity function have been thoroughly presented and discussed in [3], [8].

### B. Coupling effect between delay and angle parameters

From the expression of the MIMO ambiguity function (4), it can be seen that effects of delays and angles cannot generally be decoupled, except for two specific cases:

- $\mathbf{S}(\tau) = \lambda_s(\tau)\mathbf{1}_{N_E \times N_E}$  where  $\mathbf{1}_{N_E \times N_E}$  is a matrix of size  $N_E \times N_E$  filled with ones and  $\lambda_s(\tau)$  is a correlation function. In that case, the ambiguity function becomes:

$$A_e(\tau, \theta, \theta_c) = (\mathbf{s}_E^T(\theta_c)\mathbf{1}_{N_E \times N_E}\mathbf{s}_E^*(\theta)) \lambda_s(\tau).$$

This case arises when  $s_m(t) = s(t)$  for all  $m$ , i.e. the classic phased array where all transmitted signals are identical; it is of no interest in the MIMO framework.

- $\mathbf{S}(\tau) = \lambda_s(\tau)\mathbf{I}_{N_E}$  where  $\mathbf{I}_{N_E}$  is the identity matrix. In that case, the ambiguity function becomes:

$$A_e(\tau, \theta, \theta_c) = (\mathbf{s}_E^T(\theta_c)\mathbf{s}_E^*(\theta)) \lambda_s(\tau).$$

This arises when all cross ambiguities are equal to zero for all  $\tau$  and all auto ambiguities are identical, i.e.:

$$\int s_m(t)s_{m'}^*(t + \tau) dt = \lambda_s(\tau)\delta_{m,m'},$$

where  $\delta_{m,m'}$  is the Kronecker operator. In other words, it means that the transmitted waveforms are perfectly orthogonal.

The second case is very interesting since it implies for instance that an error in the estimated delay will not necessarily induce an error in the estimated direction. Unfortunately it cannot be exactly achieved in practice since it is not possible to generate  $N_E$  perfectly orthogonal waveforms with identical autocorrelations. It is however possible to design approximately orthogonal signals. Then, delays and angles may be approximately decoupled again. The counterpart will generally be an increase in the sidelobe level. We will now present several possible waveform families achieving this approximated orthogonality.

## III. COHERENT MIMO WAVEFORMS

In this section, we present first a general formalism for intrapulse coding of MIMO waveforms. Then we present several different coding schemes. For all the results presented in the following, the parameters used for the simulations have been set (unless differently specified) to:  $N_E = 12$  transmission antennas,  $T_p = 63.5 \mu\text{s}$ .

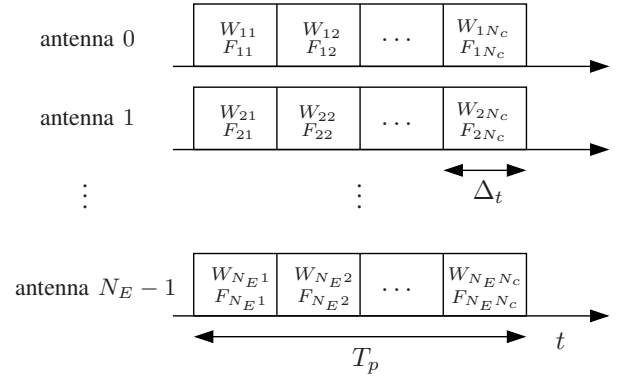


Fig. 2. General intrapulse coding scheme.

### A. Intrapulse coding formalism

We consider here that the MIMO radar transmits a pulse train. Each antenna transmits its specific waveform during one pulse, and we assume here that this waveform is identical from pulse to pulse. Therefore the orthogonality between the different waveform arises only from the intrapulse coding.

Each pulse can be decomposed into  $N_c$  time slots or “chips”. To each time slot and each antenna can be assigned specific phases and frequencies. We therefore propose the general model for intrapulse coding:

$$s_m(t) = \sum_{p=0}^{N_c-1} W_{mp} e^{j2\pi F_{mp}t} u(t - p\Delta_t),$$

where  $W_{mp}$  and  $F_{mp}$  represent the phase and the frequency associated to the signal transmitted by the antenna  $m$  during the time slot  $p$ .  $\Delta_t$  represents the duration of one chip, and  $u(t)$  represents the elementary waveform, that can be for instance a simple rectangular pulse or a linear frequency modulated signal (“chirp”). This expression permits to design at the same time waveforms with phase and/or frequency coding. Such a code is represented in figure 2. Note that the number of chips  $N_c$  can be set as desired depending on the signal to transmit. For instance, if the transmitted pulse is a chirp, then we can set  $N_c = 1$  and use a chirp for elementary pulse  $u(t)$ .

Using the vectorial notation, the transmitted signal can be expressed as:

$$\mathbf{s}(t) = (\mathbf{W} \circ \mathbf{F}(t))\mathbf{u}(t),$$

where  $\circ$  represents the Hadamard product,  $\mathbf{W}$  and  $\mathbf{F}(t)$  are matrices of size  $N_E \times N_c$  whose elements are respectively provided by  $W_{mp}$  and  $e^{j2\pi F_{mp}t}$ , and

$$\mathbf{u}(t) = [u(t) \quad u(t - \Delta_t) \quad \dots \quad u(t - (N_c - 1)\Delta_t)]^T.$$

We will now present different families of codes that can be used in MIMO radar.

### B. Circulating pulse (TDMA)

A first simple code is the circulating pulse, that consists in transmitting different cyclic permutations of the same code on the different antennas. This code can be defined by setting

$$\mathbf{W} = \mathbf{C}(\mathbf{s}) \quad \text{and} \quad \mathbf{F}(t) = \mathbf{1}_{N_E \times N_c},$$

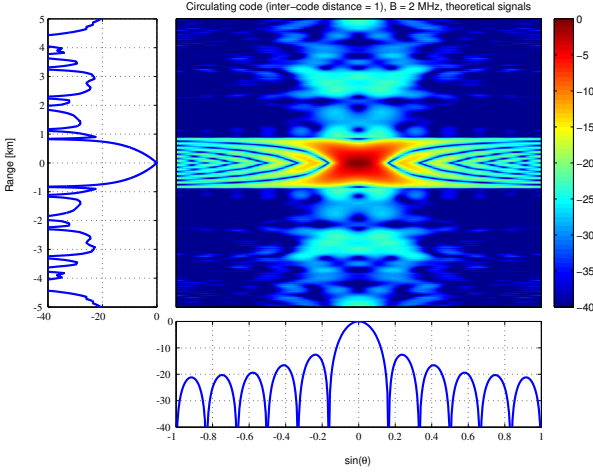


Fig. 3. Range - angle cut of the MIMO ambiguity function of the circulating pulse for  $\theta_c = 0$  with a PN sequence of length  $N_c = 127$ .  $N_E = 12$  transmission antennas.  $T_p = 63.5 \mu\text{s}$ ,  $B = 2 \text{ MHz}$ . One single antenna on receive.

where  $\mathbf{C}(s)$  is the circulant matrix built from signal code  $s$  containing  $N_c$  chips.

This code fulfills the orthogonality condition for  $\tau = 0$  if the code used presents good periodic autocorrelation features (for instance a PN sequence) but not for non zero delays, thus limiting the range resolution to that corresponding to the bandwidth of  $s$  multiplied by the number of antennas. Cuts of the resulting ambiguity function are presented in figure 3 for the target position  $\theta_c = 0$ . Let us notice that for that specific code, the transmission directivity has been obtained at the price of a loss in the range resolution.

### C. One frequency per antenna (FDMA)

Another simple case to consider is the case where all antennas transmit signals at different frequencies. This strategy corresponds to the FDMA multiplexing in digital communications. It corresponds to

$$N_c = 1, \quad \mathbf{W} = \mathbf{1}_{N_E \times 1} \quad \text{and} \quad \mathbf{F} = [0, \Delta_f, \dots, (N_E - 1)\Delta_f]^T,$$

where  $\Delta_f$  is a frequency interval larger or equal to the signal bandwidth, i.e.  $\Delta_f \geq B$  with  $B$  the bandwidth of  $u(t)$ . Clearly the transmitted signals are orthogonal since they do not share the same frequency domains. But this is not enough to get perfect delay - angle decoupling. Indeed, if the initial phases are the same for the different signals, then the signal transmitted by the array at a given time instant  $t$  is the vector

$$[1, e^{j2\pi\Delta_f t}, \dots, e^{j2\pi(N_E-1)\Delta_f t}]^T$$

which corresponds to a direction  $\theta = \text{asin}(2\Delta_f t)$  when considering a linear array with antennas separated by  $\lambda/2$ . Therefore this coding scheme resorts to a fast sweeping of the different angular directions during the pulse duration. This also means that the signal received in direction  $\theta$  at a given time  $t$  is similar to the signal received in direction 0 at time  $t' = \sin(\theta)/(2\Delta_f)$ , thus leading to a noticeable delay - angle

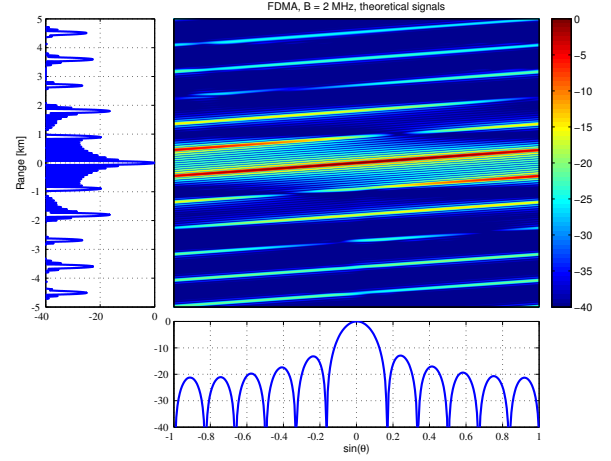


Fig. 4. Range - angle cut of the MIMO ambiguity function for the FDMA coding scheme with elementary bandwidth  $B = 166.67 \text{ kHz}$  (i.e. total bandwidth  $B_{tot} = 2 \text{ MHz}$ ).  $N_E = 12$  transmission antennas.  $T_p = 100 \mu\text{s}$ .

coupling along the line  $\tau = 1/(2\Delta_f)\sin(\theta)$ , or, by replacing the delay by the range,  $d = c/(4\Delta_f)\sin(\theta)$  where the range is  $d = c\tau/2$  and  $c$  is the wave velocity. This coupling can be easily seen in figure 4 that presents the MIMO ambiguity function for the FDMA coding scheme with  $B = 166.67 \text{ kHz}$ , where  $\Delta_f$  has been set to  $B$ . Interestingly we can notice that the mainlobe width corresponds to the overall bandwidth used, equal to  $B_{tot} = 2 \text{ MHz}$ .

### D. One phase code per antenna (CDMA)

We have seen that perfect orthogonality is desired to remove the range/angle coupling. Even though this perfect orthogonality cannot be obtained, it is possible to consider code families that present features close to this orthogonality. For instance, some classes of codes have been designed in digital communications to exhibit very good autocorrelation and crosscorrelations properties. This is the case for instance for the Gold codes [9]. Although the good properties of these codes are theoretically obtained for periodic correlations, they remain interesting in the considered aperiodic case.

For phase codes, the number of chips  $N_c$  is set so as to provide a given desired bandwidth. Then the frequency matrix is simply set to  $\mathbf{F} = \mathbf{1}_{N_E \times N_c}$  while the phase matrix  $\mathbf{W}$  is provided by the considered phase codes. The ambiguity function for the Gold codes is presented in figure 5. We can notice that for this class of codes, the range/angle sidelobes are approximately uniformly spread in the range/angle plane. Therefore approximate decoupling has indeed been obtained, at the cost of a relatively high sidelobe level that may be problematic in the presence of spread clutter.

### E. Cramer-Rao-Lower-Bound ellipses

The range/angle coupling discussed previously can also be highlighted thanks to the well-known Cramer-Rao-Lower-Bound (CRLB) [10]. This CRLB is given by the inverse of

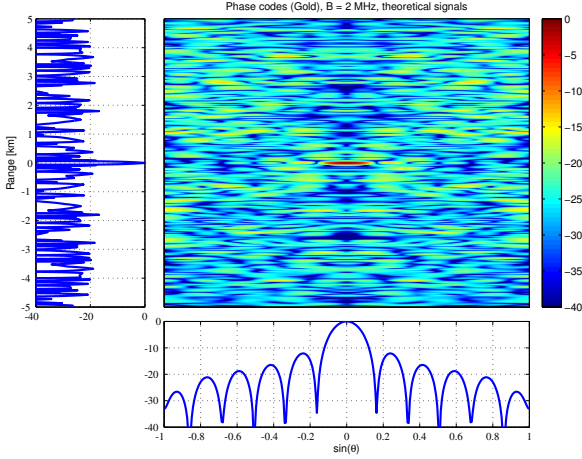


Fig. 5. Range - angle cut of the MIMO ambiguity function for the CDMA coding scheme with Gold code of length  $N_m = 127$ .  $N_t = 12$  transmission antennas.  $T_p = 100 \mu s$ ,  $B = 2.55$  MHz.

the Fisher information matrix  $\mathbf{J}$ . In radar, each term  $J_{kl}$  of this matrix can be computed from the ambiguity function by:

$$J_{kl} = -\text{SNR}_{out} \frac{\partial^2 |A_e(\tau, \theta, \theta_c)|^2}{\partial \gamma_k \partial \gamma_l},$$

where  $\gamma_k$  is one of the parameters  $\tau$ ,  $\theta$ ,  $\theta_c$ , and  $\text{SNR}_{out}$  is the SNR at the output of the MIMO processing. For the sake of simplicity, we will consider only the two parameters  $\tau$  and  $\theta$ . In that case,  $\mathbf{J}$  is a  $2 \times 2$ -matrix. Computing this matrix and the corresponding CRLB can provide insight on the range/angle coupling for a given coding scheme. Indeed the CRLB matrix defines an ellipse corresponding to the minimal possible bound that can be achieved for estimating the corresponding estimator. We present in figure 6 this ellipses for the three codes discussed in the previous sections. Note that these ellipses are computed on the code after the band-pass transmission filter which permits to limit the bandwidth for phase codes. Clearly the shapes of the ellipses differ between the codes. In particular the CRLB ellipse for the FDMA code shows a clear range/angle coupling. This coupling induces an increase of the minimal variance of the estimator in range and angle that can be achieved for this specific coding scheme. Among the three studied codes, the one producing the CRLB ellipse with the smallest surface is the CDMA code, thus allowing the best estimate for single target estimation. On the contrary this code provides the highest sidelobe level, spread over the whole ambiguity domain, which prevent against its use in strong clutter situations or for weak target detection.

#### IV. EXPERIMENTS ON A MIMO RADAR DEMONSTRATOR

Many different effects of reality are not taken into account in the theoretical data, especially material defaults like non-linear phase of microwave transmit/receive chains and antenna coupling (inducing impedance mismatch) and also non-optimal propagation like multipath. One threat with the MIMO is that a "localized" issue, for example a defective transmission

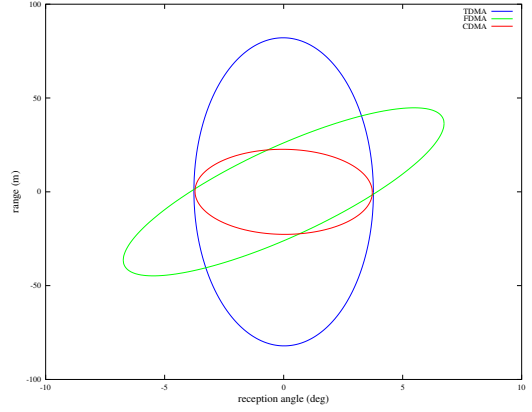


Fig. 6. CRLB ellipses in range and reception angle for the TDMA, FDMA and CDMA codes discussed previously with same parameters.

antenna, may damage the orthogonality between the related waveform and all others, and therefore induce an additive "noise" on the global ambiguity function. To measure the possible effects induced by these defaults on the MIMO ambiguity function, we proceeded experimental tests with a real MIMO radar: HYCAM.

##### A. The HYCAM platform

A multifunction MIMO radar - named HYCAM - has been designed and build by ONERA. The objective was to develop a system taking into account nowadays radar architecture but also foremost future radar concepts like MIMO. It operates in S band with a bandwidth up to 500 MHz. The antenna arrays are composed of 12 electronically steerable columns for the transmission and 16 reconfigurable mono-pulse capable columns for the reception. Up to 3 intermediate frequency signals can be simultaneously up-converted and provided to the antennas through an optical rotary joint. Consequently, this make it possible to work as real MIMO with the generation and transmission of 3 orthogonal waveforms. Once captured, the received signals are downlinked through the optical fiber, then converted, digitalized and recorded for later data analysis.

##### B. Sequential MIMO experiments

The aim of the experiments is to acquire data in the context of sequential MIMO transmission with HYCAM to a specific target simulator. The signals are generated by an Arbitrary Waveform Generator (AWG). We want to test families of 12 waveforms but since HYCAM cannot proceed more than 3 different signals simultaneously, the transmissions and acquisitions are done sequentially: each waveform is transmitted "one by one" by the related antenna. A target simulator facing HYCAM at 250 meters has the ability to apply a delay and a Doppler to the signal, such that it is possible to extract the transmitted signal from the clutter during the processing phase. The successive received signal are calibrated and summed in order to recover the equivalent MIMO situation.

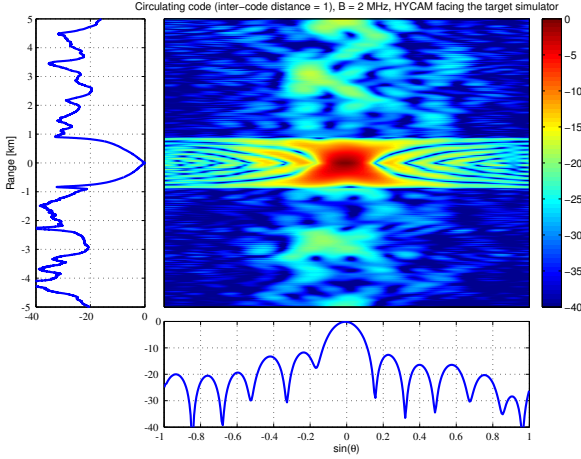


Fig. 7. Range - angle cut of the MIMO ambiguity function of the circulating pulse with a PN sequence of length  $N_c = 127$  obtained from real HYCAM data.  $N_E = 12$  transmission antennas.  $T_p = 63.5 \mu\text{s}$ ,  $B = 2$  MHz. One single antenna on receive.

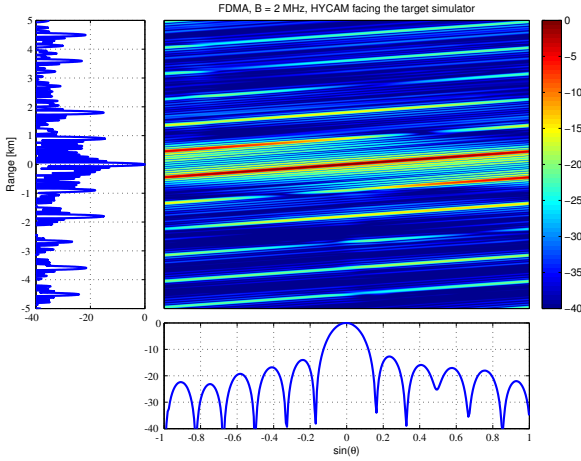


Fig. 8. Range - angle cut of the MIMO ambiguity function for the FDMA coding scheme with elementary bandwidth  $B = 166.67$  kHz (i.e. total bandwidth  $B_{tot} = 2$  MHz) obtained from real HYCAM data.  $N_E = 12$  transmission antennas.  $T_p = 100 \mu\text{s}$ .

### C. Results and analysis

The same waveform families as the ones studied in section III have been used for the experiments. The ambiguity functions measured from the acquired data are shown in figures 7, 8 and 9. They can be directly compared to theoretical figures 3, 4 and 5 respectively. Despite some slightly higher sidelobes, it is visible that experimental ambiguity functions obtained from real data are close to the theoretical ones. In fact the discrepancy is relatively small for the three waveform families, and generally limited to some local changes in the sidelobe levels. In particular their properties, such as range/angle coupling and sidelobe level, have been fairly well preserved.

## V. CONCLUSION

In this paper, we have studied the MIMO ambiguity function. We have shown that, in its general form, it implies a range/angle coupling, unless the transmitted waveforms are perfectly orthogonal. Although this perfect orthogonality is

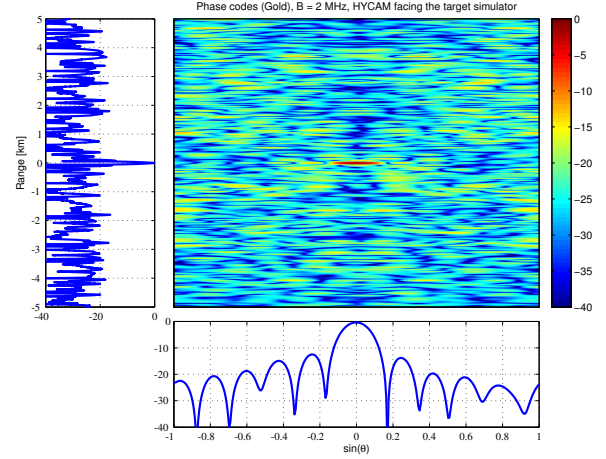


Fig. 9. Range - angle cut of the MIMO ambiguity function for the CDMA coding scheme with Gold code of length  $N_m = 127$  obtained from real HYCAM data.  $N_t = 12$  transmission antennas.  $T_p = 100 \mu\text{s}$ ,  $B = 2.55$  MHz.

assumed in most of the papers, it cannot be achieved in practice, so that range/angle coupling will always occur. We have therefore studied this feature for three different coding schemes that may take the form of a diagonal ridge in the range/angle plane, or relatively high sidelobes spread over the whole ambiguity domain. We have also shown that a quantitative insight on the range/angle coupling can be provided by CRLB ellipses. Measurements obtained from a real MIMO radar have permitted to show a fairly good match between theoretical ambiguity functions and measured ambiguity functions taking into account many transmission defaults. Finally, note that methods for generating new families of quasi-orthogonal waveforms with better range/angle coupling and/or sidelobe levels would be very relevant to produce interesting MIMO ambiguity functions.

## REFERENCES

- [1] J. Li and P. Stoica. MIMO Radar - Diversity means Superiority. In *14th Annual Workshop on Adaptive Sensor Array Processing*, 2006.
- [2] J. Li and P. Stoica. MIMO Radar with Colocated Antennas. *IEEE Signal Processing Magazine*, pages 106–114, 2007.
- [3] C.Y. Chen and P.P. Vaidyanathan. MIMO Radar Ambiguity Properties and Optimization Using Frequency-Hopping Waveforms. *IEEE Trans. on Signal Processing*, 56(12):5926–59368, 2008.
- [4] Y.I. Abramovich, G.J. Frazer, and B.A. Johnson. Noncausal Adaptive Spatial Clutter Mitigation in Monostatic MIMO radar: Fundamental Limitations. *IEEE Journal of Selected Topics in Signal Processing*, 4(1):40–54, 2010.
- [5] E. Fishler, A. Haimovich, R.S. Blum, Jr. Cimini, L.J., D. Chizhik, and R.A. Valenzuela. Spatial diversity in radars-models and detection performance. *Signal Processing, IEEE Transactions on*, 54(3):823 – 838, 2006.
- [6] A. De Maio and M. Lops. Design principles of mimo radar detectors. *Aerospace and Electronic Systems, IEEE Transactions on*, 43(3):886 – 898, 2007.
- [7] G. San Antonio, D.R. Fuhrmann, and F.C. Robey. MIMO Radar Ambiguity Functions. *IEEE Journal of Selected Topics in Signal Processing*, 1(1):167–177, 2007.
- [8] C.-Y. Chen. *Signal Processing Algorithms for MIMO Radar*. PhD thesis, California Institute of Technology, 2009.
- [9] R. Gold. Optimal binary sequences for spread spectrum multiplexing. *IEEE Trans. on Information Theory*, 13(4):619–621, 1967.
- [10] H.L. Van Trees. *Detection, Estimation and Modulation Theory, Part III*. John Wiley & Sons, 1971.